

Dynamic Attention-Guided Context Decoding for Mitigating Context Faithfulness Hallucinations in Large Language Models

Yanwen Huang^{1,2,†}, Yong Zhang^{1,†}, Ning Cheng^{1,*},
Zhitao Li¹, Shaojun Wang¹, Jing Xiao¹,

¹ Ping An Technology (Shenzhen) Co., Ltd., China

² University of Electronic Science and Technology of China
{zhangyong203, chengning211}@pingan.com.cn

Abstract

Large language models (LLMs) often suffer from context faithfulness hallucinations, where outputs deviate from retrieved information due to insufficient context utilization and high output uncertainty. Our uncertainty evaluation experiments reveal a strong correlation between high uncertainty and hallucinations. We hypothesize that attention mechanisms encode signals indicative of contextual utilization, validated through probing analysis. Based on these insights, we propose *Dynamic Attention-Guided Context Decoding (DAGCD)*, a lightweight framework that integrates attention distributions and uncertainty signals in a single-pass decoding process. Experiments across QA datasets demonstrate DAGCD’s effectiveness, achieving significant improvements in faithfulness and robustness while maintaining computational efficiency.

1 Introduction

Large Language Models (LLMs) (Brown et al., 2020; Achiam et al., 2023; Touvron et al., 2023) excel at generating fluent and contextually relevant responses. However, they often struggle with producing factually accurate outputs, particularly when relying on external information (Vu et al., 2023). Retrieval-Augmented Generation (RAG) (Lewis et al., 2020; Guu et al., 2020) mitigates this by grounding outputs in retrieved context, making it effective for tasks like question answering and reasoning (Gao et al., 2023; Fan et al., 2024). However, models often fail to faithfully utilize retrieved context, resulting in context faithfulness hallucinations, where outputs deviate from the retrieved context (Huang et al., 2023a; Ji et al., 2023). These issues undermine RAG systems’ reliability, partic-

[†] Equal contribution.

^{*} Corresponding author.

This work was done during Yanwen Huang’s internship at Ping An Technology (Shenzhen) Co., Ltd., China.

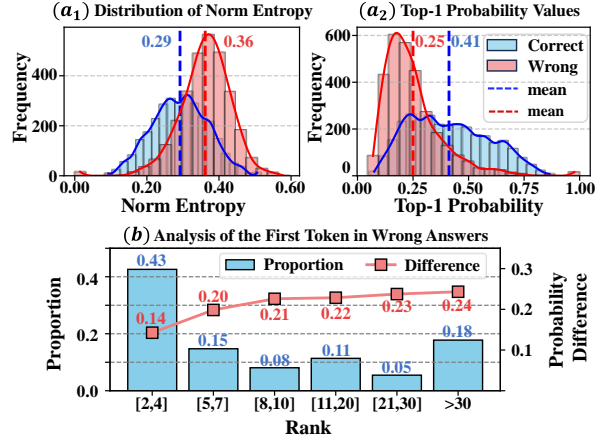


Figure 1: Analysis of generation distribution when concatenating context: (a_1, a_2) the model’s uncertainty when generating correct versus wrong answers; (b) for wrong answers, the ranking of the gold answer token in the distribution, and the probability difference between the gold answer token and the Top-1 predicted token.

ularly in high-stakes applications requiring factual accuracy (Chuang et al., 2024a).

Existing methods, such as CAD (Shi et al., 2024b) and COIECD (Yuan et al., 2024), attempt to mitigate context faithfulness hallucinations by dynamically adjusting decoding distributions through generation distribution comparisons or token-level uncertainty signals. While effective to some extent, these methods face several key limitations: limited interpretability, degraded performance when context-agnostic and context-aware outputs differ significantly, and high computational overhead due to multiple decoding passes. These issues highlight the need for lightweight and interpretable approaches that can effectively utilize retrieved context while maintaining scalability.

To further explore these issues, we analyze the relationship between output uncertainty and context faithfulness hallucinations. As shown in Figure 1, we observe a strong correlation between context hallucinations and high entropy in the generation distribution. Specifically, incorrect generations of-

ten reflect significant uncertainty through high entropy. Notably, in cases of wrong answers, context tokens corresponding to the correct answer often appear within the top-10 ranks but are assigned insufficient confidence. This indicates that the model’s internal mechanisms encode interpretable signals to indicate context utilization.

Building on our analysis and findings in interpretability studies, we hypothesize that *attention mechanisms in Transformer models encode signals indicative of contextual utilization*. Attention modules play a critical role in aligning generated tokens with their corresponding context tokens by distributing focus across input tokens (Geva et al., 2023; Jin et al., 2024b). To validate our hypothesis, we trained a probing classifier using Logistic Regression on attention distributions, achieving over 97% accuracy in distinguishing contextually relevant tokens. These results demonstrate that attention weights can serve as a lightweight and interpretable proxy for assessing the effective incorporation of retrieved evidence during generation.

Motivated by these findings, we propose Dynamic Attention-Guided Context Decoding (DAGCD), a novel algorithm to mitigate context faithfulness hallucinations. Inspired by the copy-generator framework (See et al., 2017; Xu et al., 2020b), DAGCD integrates attention weights to estimate the relevance of tokens in the retrieved context, dynamically adjusting output probabilities. Entropy-based uncertainty measures further refine these adjustments, amplifying underconfident but contextually relevant tokens. By unifying these strategies, DAGCD aligns outputs with context while maintaining computational efficiency. Our contributions are as follows:

1. **Comprehensive analysis of context faithfulness hallucinations:** We reveal a strong correlation between context faithfulness hallucinations and output uncertainty through entropy-based analysis, revealing the model’s challenges in aligning with retrieved context under high uncertainty.
2. **Attention-driven interpretability framework:** We propose *Dynamic Attention-Guided Context Decoding (DAGCD)*, leveraging attention distributions to amplify contextually relevant tokens and ensure faithful utilization of retrieved context.
3. **Lightweight and efficient decoding:** DAGCD operates in a single decoding pass, integrating attention signals and uncertainty

measures without additional overhead, achieving improved decoding efficiency.

4. **Extensive validation across datasets and models:** DAGCD outperforms greedy decoding across multiple QA datasets, achieving an average F1 score improvement of **8.95%** on pretrained models and **1.91%** on instruction-tuned models, demonstrating its robustness and scalability.

2 Why Can’t Generate Faithful Answers?

LLMs often fail to generate responses that are faithful to the concatenated context. We analyzed (1) the impact of context concatenation on output uncertainty (§2.1) and (2) the ranking of contextual answer tokens within predictions (§2.2). Our findings indicate that high output uncertainty and low confidence in contextually relevant tokens are critical factors contributing to this issue.

2.1 Uncertainty Leads to Unfaithful Answers

To assess the relationship between uncertainty and response faithfulness, we focus on two widely used metrics: entropy, which measures the overall uncertainty in the output distribution (Xu et al., 2020a; van der Poel et al., 2022; Huang et al., 2023b), and top-1 token probability, which reflects the model’s confidence in its highest-ranked prediction (Yao et al., 2023; Luo et al., 2024). Higher entropy indicates greater uncertainty, while higher top-1 probability corresponds to greater confidence in the model’s predictions.

Experimental Setup We compute the normalized entropy and top-1 token probability for the first generated token. Normalized entropy is defined as:

$$H_{\text{norm}}(P) = -\frac{\sum_{i=1}^N P_i \log P_i}{\log N}, \quad (1)$$

where P represents the probability distribution, and N denotes the vocabulary size. These metrics quantify prediction confidence, with lower entropy and higher top-1 probability reflecting greater certainty. Detailed descriptions of the datasets, models, and calculation processes are provided in Appendix A. **Results and Analysis** Figure 1 (subplots a_1 and a_2) illustrates the normalized entropy and top-1 token probability distributions for correct and wrong answers. The model exhibits higher uncertainty for wrong answers, with an average normalized entropy of 0.36 compared to 0.29 for correct cases, and a lower average top-1 probability of 0.25 compared to 0.41. Notably, a significant overlap exists

| Model | w/o context | w/ context |
|---------------------|-------------|------------|
| LLaMA2-7B | -0.43 | -0.53 |
| LLaMA2-7B-Chat | -0.27 | -0.33 |
| LLaMA2-13B | -0.30 | -0.51 |
| LLaMA2-13B-Chat | -0.26 | -0.32 |
| Mistral-7B | -0.23 | -0.22 |
| Mistral-7B-Instruct | -0.30 | -0.33 |

Table 1: Spearman correlation analysis. We examine the relationship between F1 scores (pred-ans vs. gold-ans) and norm-entropy (generation distribution) under both w/o and w/ context settings ($p \ll 0.05$ for all models).

between the entropy distributions of correct (blue) and wrong (red) cases, indicating that even correct answers often exhibit high uncertainty.

Building on this observation, we conduct a Spearman correlation analysis (Table 1), further demonstrating how uncertainty (norm-entropy of the generation distribution) negatively correlates with accuracy (F1 score between predicted and golden answers) across all models. After concatenating context, this correlation becomes even more pronounced, confirming that **uncertainty is a key factor in generating unfaithful answers**.

2.2 LLM is Actually Utilizing Context

Experimental Setup Using the wrong answer samples from §2.1, we analyze the ranking distribution of the gold answer token in the first generated distribution following context concatenation. Ranks are grouped into intervals (e.g., rank 2–4, rank 5–7, etc.), and we compute the proportion of gold answer tokens within each rank interval. Additionally, we calculate the average probability gap between the gold answer token and the top-1 token.

Results and Analysis As shown in Figure 1 (subplot *b*), when the model answers incorrectly after context concatenation, 43% of the samples have the gold answer token ranked between 2–4, and a total of 66% have the gold answer token ranked within the top 10. Moreover, the average probability gap between the gold answer token and the top-1 token is relatively small: only 0.14 for ranks between 2–4 and 0.24 for ranks greater than 30. This indicates that, in most cases, the model can correctly identify the gold answer token within the context after concatenation, but it often fails to prioritize it effectively during the generation process.

The findings highlight that **in context faithfulness hallucination scenarios, the model utilizes correct context tokens but assigns them insufficient confidence, limiting their influence on the output**. This limitation underscores the model’s incomplete integration of retrieved context, prompt-

ing an exploration of how context tokens are incorporated to guide strategies for enhancing faithfulness and mitigating hallucinations.

3 Context Utilization Signal in Attention

3.1 Background and Hypothesis

Building on our findings, we focus on the attention mechanisms in Transformer models as a potential indicator of context token utilization. Attention mechanisms distribute focus across input tokens during generation, capturing the alignment between generated tokens and their corresponding context tokens (Clark et al., 2019a; Geva et al., 2023). We hypothesize that attention heads encode signals indicating the contribution of retrieved context tokens to the generation of specific outputs. This provides a lightweight and interpretable approach to understanding contextual integration.

3.2 Attention Ratio

Analyzing raw attention weights poses challenges, as attention sink often results in disproportionate focus on non-context tokens such as delimiters, introducing noise to the analysis. (Xiao et al., 2024; Clark et al., 2019b; Bondarenko et al., 2021; Son et al., 2024; Sun et al., 2024). Additionally, varying attention magnitudes across heads and layers (Jain and Wallace, 2019; Vig and Belinkov, 2019) complicate feature comparison. To address these challenges, we compute normalized attention ratios exclusively for context tokens, reducing noise and stabilizing values across layers and heads. This approach constrains features to $[0, 1]$, enabling consistent evaluation of context token importance. Formally, the attention ratio for token j during the generation step, at the h -th head in the l -th layer, is defined as:

$$r_{l,h}^j = \frac{a_{l,h}^j}{\sum_{j \in C} a_{l,h}^j} \quad (2)$$

where $a_{l,h}^j$ represents the raw attention weight assigned to token j in the context C , and $\sum_{j \in C} a_{l,h}^j$ is the total attention weight for all tokens in C . This ratio quantifies the relative importance of token j within the context for a specific attention head.

For each token j , we construct a feature vector by aggregating its attention ratios across all heads:

$$v_j = \left[r_{1,1}^j, \dots, r_{\text{num_layers}, \text{num_heads}}^j \right] \quad (3)$$

the attention ratio feature vector v_j provides a comprehensive representation of the token’s attention

| Model | ACC | AUC |
|---------------------|--------|--------|
| LLaMA2-7B | 0.9793 | 0.9925 |
| LLaMA2-7B-Chat | 0.9798 | 0.9970 |
| LLaMA2-13B | 0.9740 | 0.9935 |
| LLaMA2-13B-Chat | 0.9737 | 0.9924 |
| Mistral-7B | 0.9787 | 0.9915 |
| Mistral-7B-Instruct | 0.9756 | 0.9883 |

Table 2: Performance of the LR classifier. We report the average performance across different random seeds.

patterns, capturing its relative importance across the model’s entire architecture.

3.3 Experimental Setup and Results

To validate our hypothesis, we focused on cases where **the model’s output shifted from incorrect to correct after context concatenation**. Context tokens were labeled as positive (utilized) if they corresponded to the gold answer, and negative (non-utilized) otherwise. Using these labels, we extracted attention ratio feature vectors \mathbf{v}_j under Prompt 1 to train a Logistic Regression (LR) classifier. The classifier was evaluated across multiple Transformer-based LLMs, including LLaMA2 and Mistral models. Details on dataset construction, training, and evaluation are in Appendix B.

The LR classifier demonstrates excellent performance across all evaluated LLMs, achieving accuracy above 0.97 and AUC scores exceeding 0.99 (Table 2). These results confirm that attention ratio features effectively distinguish utilized tokens from non-utilized ones, validating the hypothesis that attention patterns encode signals of contextual utilization. This robust performance, observed across various LLaMA2 and Mistral models, including chat and instruction-tuned variants, highlights the generality of attention ratio features across different architectures and fine-tuning paradigms. Moreover, the findings emphasize the potential of attention-based features as lightweight, interpretable signals for improving RAG systems.

3.4 Generalization and Feature Analysis

To validate the robustness and generalization of the LR classifier, we conducted extensive evaluations across out-of-domain data, prompt variations, and feature contributions.

Out-of-Domain Evaluation We tested the classifier on six sub-datasets from different domains, training on five sub-datasets and evaluating on the held-out one. As shown in Figure 2, the classifier achieves an average accuracy (ACC) and area under the curve (AUC) above 0.95 across all datasets and LLMs. These results demonstrate strong gen-

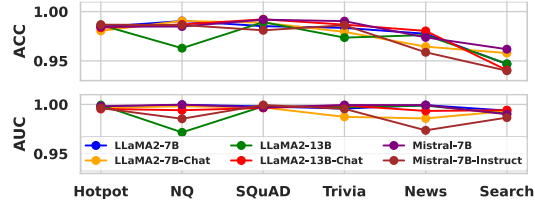


Figure 2: Out-of-domain performance of the LR classifier. One dataset is used as the test set, and the remaining datasets are used as the training set.

eralization capabilities of attention ratio features, even when applied to unseen domains.

Additional Analyses We further evaluated the robustness of attention-based features to prompt variations and analyzed the importance and characteristics of individual features. Results show that the classifier consistently performs well across prompts with minimal variation and the performance of classifier with top-K features surpasses that of using full features. Additionally, attention heads exhibit complementary behavior and data-dependent characteristics. Detailed results for these analyses are provided in Appendix C and Appendix D.

4 Method

Inspired by the copy-generation mechanism (See et al., 2017; Xu et al., 2020b), we propose **Dynamic Attention-Guided Context Decoding (DAGCD)** to migrate context faithfulness hallucinations. DAGCD leverages utilization signals to dynamically guide the generation process, focusing on relevant contextual tokens. It integrates three steps: detecting utilized context tokens during inference (§4.1), constructing a utilization distribution (§4.2), and adjusting the generation probabilities to enhance contextual relevance (§4.3).

4.1 Context Utilization Detection

Context Utilization Detector In Section 3.4, we observed that the LR classifier trained using attention ratios from all attention heads did not generalize as effectively as the LR classifier trained with top-K features. Consequently, we selected the LR model trained with top-K features as the *Context Utilization Detector*. The set of attention heads corresponding to the top-K features used for training is denoted as $A = [A_{l_1, h_1}, A_{l_2, h_2}, \dots, A_{l_K, h_K}]$, where each head A_{l_k, h_k} is associated with a feature coefficient c_k (for all models, we set $K = 10$).

Feature Data Collection As illustrated in Figure 3, the attention distribution at the current decoding step is obtained by extracting the last row of the at-

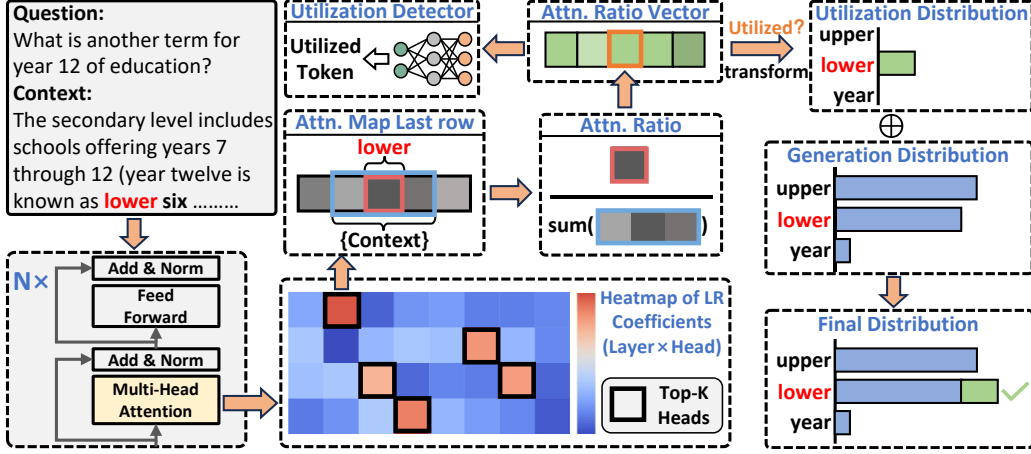


Figure 3: The illustration of the generation process of our proposed DAGCD method.

tention map for each head $A_{l_k, h_k} \in A$. To focus on relevant information, we filter out non-contextual tokens, such as prompts and special symbols (e.g., ‘\n’, ‘<unk>’). The top-K feature vector for each token j is then computed as:

$$\mathbf{v}_j^{(K)} = [r_{l_1, h_1}^j, r_{l_2, h_2}^j, \dots, r_{l_K, h_K}^j] \quad (4)$$

Finally, the feature vector $\mathbf{v}_j^{(K)}$ is fed into the detector, which identifies the set of context tokens actively utilized at the current decoding step.

4.2 Utilization Distribution Construction

The context utilization detector identifies utilized tokens but does not quantify the degree of utilization for each token. To address this, we aggregate the attention ratios from different attention heads, weighted by their normalized feature coefficients w_k , to compute a utilization score for each token. Formally, the utilization score s_j for token j is defined as:

$$s_j = \sum_{k=1}^K (r_{l_k, h_k}^j \times w_k), \quad w_k = \frac{c_k}{\sum_{k=1}^K c_k} \quad (5)$$

The feature coefficient reflects the significance of each attention head, with positive values indicating a higher likelihood of token utilization and negative values suggesting a reduced likelihood. The utilization distribution is then constructed based on the utilization scores of individual tokens:

$$\mathbf{U} = [u_1, u_2, \dots, u_N], \quad u_i = \frac{s_i}{\sum_{j=1}^N s_j} \quad (6)$$

where u_i represents the normalized utilization score for token i . Here, N denotes the size of the vocabulary, and $s_i = 0$ for tokens either absent from the context or not utilized, resulting in $u_i = 0$ for such tokens.

4.3 Generate More Faithful Answers

Building on the utilization signals and the utilization distribution, DAGCD refines the generation process by dynamically adjusting token probabilities to prioritize contextually relevant tokens.

Adjustment Triggering At each decoding step, DAGCD checks if utilized tokens are detected by the *Context Utilization Detector*. If detected, their probabilities are amplified; otherwise, or during termination conditions (e.g., when the top-1 token is ‘\n’), the probabilities remain unchanged.

Dynamic Scaling of Adjustments The intensity of adjustments is guided by the model’s output uncertainty, measured as the normalized entropy $H_{\text{norm}}(P)$ of the generation distribution, as defined in Equation 1. High entropy indicates greater uncertainty and a higher risk of generating contextually inconsistent responses. Since our analysis shows that entropy correlates with uncertainty but does not establish a direct numerical relationship, we introduce a scaling factor α , which compensates for model-specific entropy variations.

Top-Rank Filtering and Distribution Adjustment To enhance the reliability of generation adjustments, our approach incorporates a top-rank restriction, ensuring modifications focus on plausible tokens. Specifically, we define U_{top} as the subset of the utilization distribution U corresponding to tokens ranked within the top- R positions of the generation distribution. This design addresses challenges similar to those highlighted in prior work (Li et al., 2023; Chuang et al., 2024b), while specifically leveraging the observation that correct context tokens are typically found within the top-rank set, even when the model produces incorrect answers. Restricting adjustments to U_{top} reduces the risk of amplifying irrelevant or nonsensical tokens,

thereby maintaining the output’s integrity.

Under this framework, adjustments are applied only when utilized tokens in U_{top} overlap with the top-rank set of the generation distribution. The adjusted generation distribution P' is computed as:

$$P' = P + \alpha H_{\text{norm}}(P) \cdot U_{\text{top}} \quad (7)$$

where P is the original generation distribution, and $\alpha H_{\text{norm}}(P)$ scales the adjustment intensity dynamically based on the normalized entropy $H_{\text{norm}}(P)$ of the entire generation distribution.

5 Experiments

5.1 Experimental Setup

Models We conducted experiments on LLaMA and Mistral, including LLaMA2 (7B, 13B, 7B-Chat, 13B-chat) (Touvron et al., 2023) and Mistral (7B, 7B-Instruct) (Jiang et al., 2023).

Datasets We conducted experiments on seven open-book question-answering (QA) datasets, representing a variety of QA tasks. These include multi-hop reasoning datasets (HotpotQA (Yang et al., 2018)), long-form retrieval-based QA datasets (TriviaQA (Joshi et al., 2017) and SearchQA (Dunn et al., 2017)), single-paragraph extraction tasks (SQuAD (Rajpurkar et al., 2016) and NewsQA (Trischler et al., 2017)), and document-level QA datasets (NQ (Kwiatkowski et al., 2019)). All datasets are formatted in the unified schema provided by the MrQA repository (Fisch et al., 2019). Additionally, we used the artificially constructed NQ-swap dataset (Longpre et al., 2021), designed to simulate conflicting or ambiguous scenarios by replacing entities. Detailed descriptions see Appendix F.3.

Baselines We compare the proposed DAGCD method with three decoding strategies: Greedy Decoding, CAD (Shi et al., 2024b), and COIECD (Yuan et al., 2024). CAD and COIECD are specifically designed to mitigate context faithfulness hallucination.

Implementation Details For DAGCD, the scaling factor α is set to 2 for pretrained models and 4 for instruction-tuned models to account for entropy variations. The logistic regression classifier and utilization distribution are computed using the top-10 attention heads, with adjustments restricted to the top-10 ranked tokens (U_{top}). Further details on prompts, decoding strategies, and baseline configurations are provided in Appendix F.4 and F.5.

Metrics Consistent with prior work (Jin et al., 2024a; Yuan et al., 2024; Wang et al., 2024), we

use EM and F1 score metrics to evaluate the performance of the models on open-domain QA datasets.

5.2 Model Performance Comparison

Table 3 demonstrates the effectiveness of DAGCD across diverse QA datasets and model configurations. We summarize the findings based on datasets and model characteristics. Additionally, we evaluated DAGCD on summarization tasks, and the results demonstrate that DAGCD also achieves improvements (detailed results see Appendix F.6).

5.2.1 Dataset-Level Observations

DAGCD achieves consistent improvements across diverse QA tasks, including multi-hop reasoning, long-form retrieval, and document-level QA.

HotpotQA, TriviaQA, SearchQA: DAGCD demonstrates strong performance in tasks requiring multi-paragraph reasoning and long-form retrieval. It achieves the highest gains on HotpotQA with a 10.02% EM and 9.05% F1 improvement on Mistral-7B. Additionally, DAGCD outperforms CAD and COIECD on TriviaQA and SearchQA, with significant improvements across different models.

SQuAD, NewsQA, NQ: DAGCD demonstrates robust performance in single-paragraph and document-level tasks. On NQ, it achieves a 24.06% EM and 21.36% F1 increase on Mistral-7B compared to greedy decoding, while delivering consistent gains across SQuAD and NewsQA datasets.

NQ-Swap: In adversarial scenarios simulated by NQ-Swap, DAGCD achieves significant improvements, including 30.10% EM and 24.35% F1 gains on Mistral-7B, underscoring its robustness in challenging conditions.

5.2.2 Model-Level Observations

DAGCD demonstrates broad applicability across different model families, sizes, and tuning variants.

Model Families: DAGCD consistently improves performance across both LLaMA and Mistral families. On Mistral-7B, DAGCD achieves an average EM of 59.54 and an average F1 of 69.69, outperforming greedy decoding by 12.99% and 13.58%, respectively. LLaMA2 models also benefit significantly, on LLaMA2-7B, with average F1 improvements of 6.91% over greedy decoding.

Model Sizes: DAGCD improves performance across models of varying model sizes, achieving an average EM and F1 increase of 6.77% and 6.91% on LLaMA2-7B, and 5.63% and 6.35% on LLaMA2-13B, respectively.

| Dataset | Decoding | HotpotQA | | TriviaQA | | SearchQA | | SQuAD | | NewsQA | | NQ | | NQ-swap | | Average | |
|---------------------|--------------|--------------|--------------|--------------|--------------|--------------|--------------|--------------|--------------|--------------|--------------|--------------|--------------|--------------|--------------|--------------|--------------|
| | | EM | F1 |
| | | LLaMA2-7B | Regular | <u>44.74</u> | <u>54.71</u> | 55.28 | 68.01 | 54.21 | 59.24 | 39.90 | 52.61 | 32.93 | 45.46 | <u>38.85</u> | <u>50.59</u> | 36.03 | 36.62 |
| CAD | 44.13 | | 54.49 | 55.26 | 68.04 | 54.14 | 59.21 | 38.35 | 51.12 | 31.74 | 43.70 | 38.14 | 48.58 | <u>36.11</u> | <u>36.69</u> | 42.55 | 51.69 |
| COIECD | 42.03 | | 51.48 | <u>57.04</u> | <u>70.06</u> | 57.03 | 63.14 | <u>40.93</u> | <u>54.78</u> | <u>34.40</u> | <u>48.48</u> | 38.79 | <u>51.69</u> | 34.98 | 35.63 | <u>43.60</u> | <u>53.61</u> |
| OURs | 47.67 | | 57.87 | 58.46 | 71.42 | <u>55.04</u> | <u>60.35</u> | 49.00 | 61.04 | 36.70 | 49.29 | 48.10 | 60.71 | 54.33 | 54.95 | 49.90 | 59.38 |
| LLaMA2-7B-Chat | Regular | <u>53.33</u> | <u>67.41</u> | <u>71.72</u> | <u>76.83</u> | 54.19 | 58.11 | 67.69 | 78.70 | 39.41 | 53.90 | 50.47 | 65.48 | 67.98 | 68.78 | 57.83 | 67.03 |
| | CAD | 52.86 | 67.16 | 71.70 | 76.83 | 54.16 | 58.11 | 65.89 | 77.91 | 38.46 | 53.26 | 48.89 | 65.00 | 68.04 | 68.85 | 57.14 | 66.73 |
| | COIECD | 53.14 | 67.03 | 72.26 | 77.33 | 55.04 | 58.98 | <u>68.32</u> | <u>79.56</u> | <u>40.00</u> | <u>54.55</u> | 52.39 | <u>66.84</u> | <u>69.48</u> | <u>70.13</u> | 58.66 | <u>67.77</u> |
| | OURs | 55.26 | 68.65 | 70.05 | 76.56 | 54.70 | 58.57 | 68.60 | 79.65 | 40.38 | 54.72 | <u>51.75</u> | 66.93 | 69.50 | 70.30 | <u>58.61</u> | 67.91 |
| LLaMA2-13B | Regular | <u>52.36</u> | <u>63.40</u> | 58.25 | 69.95 | <u>63.22</u> | <u>68.33</u> | 51.64 | 64.57 | 30.84 | 40.11 | 42.26 | 54.08 | 49.02 | 49.59 | 49.66 | 58.58 |
| | CAD | 51.53 | 63.11 | 58.25 | 69.92 | 63.13 | 68.32 | 49.94 | 63.44 | 29.94 | 39.04 | 41.40 | 52.27 | <u>49.07</u> | <u>49.63</u> | 49.04 | 57.96 |
| | COIECD | 50.21 | 60.96 | 59.19 | 71.49 | 65.97 | 71.00 | <u>52.73</u> | <u>65.93</u> | 35.66 | 50.58 | <u>42.35</u> | <u>54.37</u> | 48.35 | 48.84 | <u>50.64</u> | <u>60.45</u> |
| | OURs | 53.86 | 65.25 | 59.65 | 72.07 | 61.41 | 67.08 | 57.36 | 69.85 | <u>33.52</u> | <u>42.81</u> | 55.34 | 71.23 | 65.86 | 66.19 | 55.29 | 64.93 |
| LLaMA2-13B-Chat | Regular | 55.01 | 69.92 | 74.58 | <u>79.35</u> | 67.08 | <u>71.96</u> | 68.26 | 79.45 | 40.20 | 55.11 | 53.49 | 69.18 | 60.69 | 61.77 | 59.90 | 69.53 |
| | CAD | 54.44 | 69.66 | 74.58 | 79.37 | 67.01 | 71.95 | 66.77 | 78.70 | 39.44 | 54.44 | 52.89 | 68.63 | 60.83 | 61.92 | 59.42 | 69.24 |
| | COIECD | <u>56.15</u> | <u>70.43</u> | <u>73.87</u> | 78.96 | <u>67.28</u> | 71.93 | 68.49 | 80.39 | <u>40.75</u> | <u>56.16</u> | <u>53.69</u> | <u>69.81</u> | <u>62.47</u> | <u>63.21</u> | <u>60.39</u> | <u>70.13</u> |
| | OURs | 58.22 | 71.99 | 73.55 | 79.11 | 68.19 | 72.73 | 69.83 | 88.88 | 40.77 | 56.54 | 55.34 | 71.24 | 64.30 | 65.42 | 61.46 | 72.27 |
| Mistral-7B | Regular | <u>53.41</u> | <u>64.36</u> | 59.45 | 68.39 | <u>63.79</u> | 67.77 | 44.19 | 56.11 | 31.51 | 38.94 | 33.74 | 51.18 | 39.80 | 46.04 | 46.56 | 56.11 |
| | CAD | 41.57 | 56.01 | <u>57.88</u> | 67.48 | 63.64 | 68.65 | 34.08 | 47.55 | 25.78 | 35.37 | 23.18 | 41.46 | 26.96 | 35.97 | 39.01 | 50.36 |
| | COIECD | 46.43 | 58.32 | 44.30 | 51.77 | 54.82 | 59.17 | <u>50.50</u> | <u>60.98</u> | <u>40.05</u> | <u>52.78</u> | <u>42.12</u> | <u>56.58</u> | <u>59.53</u> | <u>61.89</u> | <u>48.25</u> | <u>57.36</u> |
| | OURs | 63.43 | 73.41 | 57.10 | 72.01 | 64.71 | 70.62 | 62.44 | 73.86 | 41.41 | 55.00 | 57.80 | 72.54 | 69.90 | 70.39 | 59.54 | 69.69 |
| Mistral-7B-Instruct | Regular | 58.70 | 72.18 | 69.64 | 75.61 | 44.42 | 49.63 | 67.28 | 79.37 | 39.79 | 54.72 | 52.29 | 66.93 | 66.90 | 67.83 | <u>57.00</u> | 66.61 |
| | CAD | 49.30 | 64.81 | 70.23 | 75.95 | <u>45.42</u> | <u>50.96</u> | 59.97 | 72.92 | 34.97 | 51.90 | 42.63 | 58.49 | 52.04 | 53.75 | 50.65 | 61.25 |
| | COIECD | <u>59.74</u> | <u>72.59</u> | 64.92 | 72.15 | 37.09 | 42.66 | 68.45 | 81.03 | <u>40.84</u> | <u>55.96</u> | <u>53.54</u> | <u>68.72</u> | 72.81 | 73.81 | 56.77 | <u>66.70</u> |
| | OURs | 60.77 | 73.82 | <u>69.70</u> | <u>75.96</u> | 47.17 | 52.65 | <u>68.29</u> | <u>80.74</u> | 40.85 | 56.01 | 54.69 | 69.81 | <u>71.27</u> | <u>72.10</u> | 58.96 | 68.73 |

Table 3: Performance comparison of different decoding methods. All baselines are reproduced under the same settings. **Bold** indicates the best performance, and underlined indicates the second-best performance.

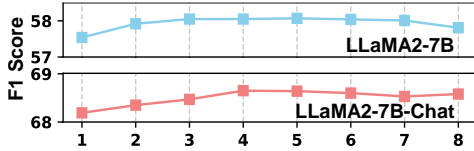


Figure 4: The impact of different α values on the performance of our method (fixed top-rank = 10).

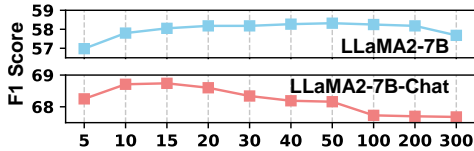


Figure 5: The impact of different Top-Rank constraint on the performance of DAGCD (fixed $\alpha = 2$ and 4).

Instruction-Tuned Models: DAGCD consistently achieves performance gains across instruction-tuned models, surpassing all baselines with the highest average EM and F1 scores.

5.3 Ablation Study

Impact of Different α We evaluated the impact of different values of α on model performance with the top-rank fixed at 10. The results, presented in Figure 4, indicate that α determines the adjustment intensity applied to the original generation distribution. For pretrained models, optimal performance is achieved at $\alpha = 2$, whereas for Chat models, the best performance is observed at $\alpha = 4$.

Impact of Different Top-Rank We evaluated F1 score variations under different top-rank filtering constraints on HotpotQA. As shown in Figure 5, top-rank filtering reduces false positives, with performance initially improving as constraints loosen,

then declining when overly relaxed.

Additional results and performance variations under different prompts in Appendix F.7 and F.8.

6 Discussion and Analysis

6.1 Dynamic Decoding: Real-Time Efficiency Without Post-Generation Correction

Post-generation correction methods, such as CAD (Shi et al., 2024b) and COIECD (Yuan et al., 2024), improve contextual alignment but often rely on multi-step processes, resulting in significant computational overhead. In contrast, our **dynamic decoding** approach integrates context adjustments directly into the generation process, providing both efficiency and real-time optimization.

Lightweight Context Utilization Detector Using a logistic regression-based Context Utilization Detector, our method enables real-time adjustments with minimal computational overhead. This detector is efficient compared to resource-intensive alternatives, such as integrated gradients or exhaustive attention head manipulation.

Single-Pass Decoding with Real-Time Faithfulness Optimization By integrating the Context Utilization Detector directly into the decoding process, our method eliminates redundant steps such as output comparisons or external consistency checks. During generation, attention-based context utilization signals are leveraged in real time to proactively enhance faithfulness. This single-step strategy ensures that the output remains aligned with the input context without requiring additional post-

processing, while maintaining the theoretical time complexity of regular decoding.

6.2 Interpretability Through Attention: Insights into Context Utilization

By systematically analyzing attention mechanisms, our approach uncovers how retrieved context influences the generation process and provides interpretable insights into the model’s behavior. **Feature-Based Attention Analysis:** Using naturally occurring cases (e.g., failure in closed-book settings but success in open-book settings), we systematically isolate attention patterns that are indicative of context utilization. A logistic regression model trained on these patterns identifies the most relevant attention heads with high accuracy, providing a quantitative measure of each head’s contribution to context alignment.

Transparent Decision-Making: The feature coefficients of the logistic regression model directly map to the importance of specific attention heads. This transparency allows for intuitive interpretation, making it clear which heads are most responsible for leveraging context tokens during generation.

7 Related Work

7.1 Context Faithfulness Hallucination

Current solutions to context faithfulness hallucination primarily focus on detection and mitigation. For detection, Lei et al. (Lei et al., 2023) proposed a post-generation editing strategy that uses natural language inference to classify and revise hallucinated segments in generated content. Choi et al. (Choi et al., 2023) introduced Knowledge-Constrained Decoding, which detects hallucinations at the token level during generation and reweights token distributions to guide output. Similarly, Chuang et al. (Chuang et al., 2024a) proposed Lookback Lens Guided Decoding, which selects the most faithful output among multiple candidates to improve consistency.

For mitigation, CAD (Shi et al., 2024b) compares outputs with and without concatenated context to enhance contextual adherence, while COIECD (Yuan et al., 2024) improves upon CAD by incorporating entropy-based constraints to balance context usage. Wang et al. (Wang et al., 2024) further introduced ADACAD, which dynamically adjusts token-level adherence using divergence between contextual and non-contextual outputs.

While effective, most existing methods face limitations such as high computational overhead and

reliance on multiple decoding passes. In this work, we propose a real-time solution that integrates context utilization signals directly into the decoding process, achieving efficient and faithful generation without additional processing steps.

7.2 Attention Mechanisms and Interpretability

The attention mechanism provides valuable insights into how models prioritize different parts of an input sequence (Clark et al., 2019a; Geva et al., 2023) and has become central to understanding Transformer-based LLMs (Vashishth et al., 2019; Hao et al., 2021; Zhao et al., 2024). In LLMs, attention heads often perform distinct roles, such as capturing syntactic dependencies or aligning semantic relationships (Olsson et al., 2022; Zheng et al., 2024; Jin et al., 2024b).

Recent studies have also explored the collaborative behavior of attention heads. For instance, the retrieval head framework (Wu et al., 2024) identifies heads that collectively retrieve relevant tokens, while cutting-off-heads (Jin et al., 2024b) highlights critical heads through systematic ablation. Gradient-based methods like IRCAN (Shi et al., 2024a) further investigate the contributions of attention scores and neurons to model outputs.

Unlike prior work that focuses on individual heads or neurons, our study examines the collaborative patterns among multiple attention heads. By analyzing how attention mechanisms collectively utilize contextual tokens, we provide a holistic view of their role in aligning outputs with user-provided context, offering new insights into Transformer-based model behavior.

8 Conclusion

In this paper, we address context faithfulness hallucinations in LLMs by proposing Dynamic Attention-Guided Context Decoding (DAGCD), a lightweight framework that integrates attention distributions and entropy-based uncertainty signals to amplify contextually relevant tokens during generation. Our analysis revealed a strong correlation between high uncertainty and hallucinations, and probing experiments validated that attention mechanisms encode signals indicative of contextual utilization. Experiments across multiple QA datasets demonstrated that DAGCD achieves consistent improvements in context faithfulness, robustness, and scalability, providing an effective solution for context-sensitive generation tasks.

Limitations

Dependency on Classifier Accuracy and Robustness to Noisy Contexts DAGCD relies on an attention-ratio based classifier to assess the relevance of context tokens during generation. While the classifier demonstrates high accuracy across datasets and models, its performance may degrade in scenarios with extremely long contexts, complex dialogues, or noisy inputs. Misclassifications in these cases could lead to incorrect adjustments, potentially amplifying irrelevant tokens or diminishing the contribution of critical ones. Similarly, the method’s robustness to adversarial or noisy contexts with misleading or irrelevant information remains an open challenge. Enhancing the classifier’s resilience and incorporating mechanisms to filter or downweight adversarial noise could further strengthen DAGCD’s applicability in real-world scenarios.

Scaling Factor Adjustment for Model Characteristics The scaling factor α introduced in DAGCD needs to be adjusted based on the characteristics of different models. Although our study shows a strong correlation between entropy-guided uncertainty measures and the model’s uncertainty during generation, it does not establish a precise quantitative relationship. This limitation necessitates empirical calibration of the scaling factor for each model to ensure effective adjustments. Such calibration ensures that the method compensates for model-specific entropy variations, but it may introduce additional computational overhead during deployment.

Generalization Across Tasks and Domains Our evaluation primarily focuses on QA tasks, leaving the generalization of DAGCD to other tasks, such as summarization or dialogue generation, unexplored. The attention-ratio based classifier, optimized for QA datasets, may require additional fine-tuning or redesign to handle different output structures and task-specific challenges. Extending the method to diverse domains and tasks could further validate its robustness and scalability.

References

Josh Achiam, Steven Adler, Sandhini Agarwal, Lama Ahmad, Ilge Akkaya, Florencia Leoni Aleman, Diogo Almeida, Janko Altenschmidt, Sam Altman, Shyamal Anadkat, et al. 2023. *Gpt-4 technical report*. *ArXiv*.

Yelysei Bondarenko, Markus Nagel, and Tijmen Blankevoort. 2021. *Understanding and overcoming the challenges of efficient transformer quantization*. In *Proceedings of the 2021 Conference on Empirical Methods in Natural Language Processing*, pages 7947–7969, Online and Punta Cana, Dominican Republic. Association for Computational Linguistics.

Tom B Brown, Benjamin Mann, Nick Ryder, Melanie Subbiah, Jared Kaplan, Prafulla Dhariwal, Arvind Neelakantan, Pranav Shyam, Girish Sastry, Amanda Askell, et al. 2020. Language models are few-shot learners. In *Advances in Neural Information Processing Systems*, volume 33, pages 1877–1901.

Sehyun Choi, Tianqing Fang, Zhaowei Wang, and Yangqiu Song. 2023. *KCTS: Knowledge-constrained tree search decoding with token-level hallucination detection*. In *Proceedings of the 2023 Conference on Empirical Methods in Natural Language Processing*, pages 14035–14053, Singapore. Association for Computational Linguistics.

Yung-Sung Chuang, Linlu Qiu, Cheng-Yu Hsieh, Ranjay Krishna, Yoon Kim, and James R. Glass. 2024a. *Lookback lens: Detecting and mitigating contextual hallucinations in large language models using only attention maps*. In *Proceedings of the 2024 Conference on Empirical Methods in Natural Language Processing*, pages 1419–1436, Miami, Florida, USA. Association for Computational Linguistics.

Yung-Sung Chuang, Yujia Xie, Hongyin Luo, Yoon Kim, James R. Glass, and Pengcheng He. 2024b. *Dola: Decoding by contrasting layers improves factuality in large language models*. In *The Twelfth International Conference on Learning Representations*.

Kevin Clark, Urvashi Khandelwal, Omer Levy, and Christopher D. Manning. 2019a. *What does BERT look at? an analysis of BERT’s attention*. In *Proceedings of the 2019 ACL Workshop BlackboxNLP: Analyzing and Interpreting Neural Networks for NLP*, pages 276–286, Florence, Italy. Association for Computational Linguistics.

Kevin Clark, Urvashi Khandelwal, Omer Levy, and Christopher D. Manning. 2019b. *What does BERT look at? an analysis of BERT’s attention*. In *Proceedings of the 2019 ACL Workshop BlackboxNLP: Analyzing and Interpreting Neural Networks for NLP*, pages 276–286.

Matthew Dunn, Levent Sagun, Mike Higgins, V Ugur Guney, Volkan Cirik, and Kyunghyun Cho. 2017. *Searchqa: A new q&a dataset augmented with context from a search engine*. *arXiv preprint arXiv:1704.05179*.

Wenqi Fan, Yajuan Ding, Liang bo Ning, Shijie Wang, Hengyun Li, Dawei Yin, Tat-Seng Chua, and Qing Li. 2024. *A survey on rag meeting llms: Towards retrieval-augmented large language models*. In *Knowledge Discovery and Data Mining*.

- Shangbin Feng, Vidhisha Balachandran, Yuyang Bai, and Yulia Tsvetkov. 2023. [FactKB: Generalizable factuality evaluation using language models enhanced with factual knowledge](#). In *Proceedings of the 2023 Conference on Empirical Methods in Natural Language Processing*, pages 933–952, Singapore. Association for Computational Linguistics.
- Adam Fisch, Alon Talmor, Robin Jia, Minjoon Seo, Eunsol Choi, and Danqi Chen. 2019. [MRQA 2019 shared task: Evaluating generalization in reading comprehension](#). In *Proceedings of the 2nd Workshop on Machine Reading for Question Answering*, pages 1–13, Hong Kong, China. Association for Computational Linguistics.
- Yunfan Gao, Yun Xiong, Xinyu Gao, Kangxiang Jia, Jinliu Pan, Yuxi Bi, Yi Dai, Jiawei Sun, Qianyu Guo, Meng Wang, and Haofen Wang. 2023. [Retrieval-augmented generation for large language models: A survey](#). *ArXiv*, abs/2312.10997.
- Mor Geva, Jasmijn Bastings, Katja Filippova, and Amir Globerson. 2023. [Dissecting recall of factual associations in auto-regressive language models](#). In *Proceedings of the 2023 Conference on Empirical Methods in Natural Language Processing*, pages 12216–12235, Singapore. Association for Computational Linguistics.
- Kelvin Guu, Kenton Lee, Zora Tung, Panupong Pasupat, and Mingwei Chang. 2020. [Retrieval augmented language model pre-training](#). In *Proceedings of the 37th International Conference on Machine Learning*, volume 119 of *Proceedings of Machine Learning Research*, pages 3929–3938. PMLR.
- Yaru Hao, Li Dong, Furu Wei, and Ke Xu. 2021. Self-attention attribution: Interpreting information interactions inside transformer. In *Proceedings of the AAAI Conference on Artificial Intelligence*, volume 35, pages 12963–12971.
- Lei Huang, Weijiang Yu, Weitao Ma, Weihong Zhong, Zhangyin Feng, Haotian Wang, Qianglong Chen, Weihua Peng, Xiaocheng Feng, Bing Qin, et al. 2023a. A survey on hallucination in large language models: Principles, taxonomy, challenges, and open questions. *ACM Transactions on Information Systems*.
- Yuheng Huang, Jiayang Song, Zhijie Wang, Huaming Chen, and Lei Ma. 2023b. [Look before you leap: An exploratory study of uncertainty measurement for large language models](#). *ArXiv*, abs/2307.10236.
- Sarthak Jain and Byron C. Wallace. 2019. [Attention is not explanation](#). In *Proceedings of the 2019 Conference of the North American Chapter of the Association for Computational Linguistics: Human Language Technologies, Volume 1 (Long and Short Papers)*, pages 3543–3556, Minneapolis, Minnesota. Association for Computational Linguistics.
- Ziwei Ji, Nayeon Lee, Rita Frieske, Tiezheng Yu, Dan Su, Yan Xu, Etsuko Ishii, Ye Jin Bang, Andrea Madotto, and Pascale Fung. 2023. [Survey of hallucination in natural language generation](#). *ACM Comput. Surv.*, 55(12).
- Albert Qiaochu Jiang, Alexandre Sablayrolles, Arthur Mensch, Chris Bamford, Devendra Singh Chaplot, Diego de Las Casas, Florian Bressand, Gianna Lengyel, Guillaume Lample, Lucile Saulnier, L’elio Renard Lavaud, Marie-Anne Lachaux, Pierre Stock, Teven Le Scao, Thibaut Lavril, Thomas Wang, Timothée Lacroix, and William El Sayed. 2023. [Mistral 7b](#). *ArXiv*, abs/2310.06825.
- Zhuoran Jin, Pengfei Cao, Yubo Chen, Kang Liu, Xiaojian Jiang, Jiexin Xu, Li Qiuxia, and Jun Zhao. 2024a. [Tug-of-war between knowledge: Exploring and resolving knowledge conflicts in retrieval-augmented language models](#). In *Proceedings of the 2024 Joint International Conference on Computational Linguistics, Language Resources and Evaluation (LREC-COLING 2024)*, pages 16867–16878, Torino, Italia. ELRA and ICCL.
- Zhuoran Jin, Pengfei Cao, Hongbang Yuan, Yubo Chen, Jiexin Xu, Huaijun Li, Xiaojian Jiang, Kang Liu, and Jun Zhao. 2024b. [Cutting off the head ends the conflict: A mechanism for interpreting and mitigating knowledge conflicts in language models](#). In *Findings of the Association for Computational Linguistics ACL 2024*, pages 1193–1215, Bangkok, Thailand and virtual meeting. Association for Computational Linguistics.
- Mandar Joshi, Eunsol Choi, Daniel Weld, and Luke Zettlemoyer. 2017. [TriviaQA: A large scale distantly supervised challenge dataset for reading comprehension](#). In *Proceedings of the 55th Annual Meeting of the Association for Computational Linguistics (Volume 1: Long Papers)*, pages 1601–1611, Vancouver, Canada. Association for Computational Linguistics.
- Tom Kwiatkowski, Jennimaria Palomaki, Olivia Redfield, Michael Collins, Ankur Parikh, Chris Alberti, Danielle Epstein, Illia Polosukhin, Jacob Devlin, Kenton Lee, Kristina Toutanova, Llion Jones, Matthew Kelcey, Ming-Wei Chang, Andrew M. Dai, Jakob Uszkoreit, Quoc Le, and Slav Petrov. 2019. [Natural questions: A benchmark for question answering research](#). *Transactions of the Association for Computational Linguistics*, 7:452–466.
- Deren Lei, Yaxi Li, Mengya Hu, Mingyu Wang, and Xi Yun. 2023. [Chain of natural language inference for reducing large language model hallucinations](#). In *NeurIPS 2023 Workshop on Instruction Tuning and Instruction Following*.
- Patrick Lewis, Ethan Perez, Aleksandra Piktus, Fabio Petroni, Vladimir Karpukhin, Naman Goyal, Heinrich Küttler, Mike Lewis, Wen-tau Yih, Tim Rocktäschel, Sebastian Riedel, and Douwe Kiela. 2020. [Retrieval-augmented generation for knowledge-intensive nlp tasks](#). In *Advances in Neural Information Processing Systems*, volume 33, pages 9459–9474. Curran Associates, Inc.

- Xiang Lisa Li, Ari Holtzman, Daniel Fried, Percy Liang, Jason Eisner, Tatsunori Hashimoto, Luke Zettlemoyer, and Mike Lewis. 2023. [Contrastive decoding: Open-ended text generation as optimization](#). In *Proceedings of the 61st Annual Meeting of the Association for Computational Linguistics (Volume 1: Long Papers)*, pages 12286–12312, Toronto, Canada. Association for Computational Linguistics.
- Chin-Yew Lin. 2004. [ROUGE: A package for automatic evaluation of summaries](#). In *Text Summarization Branches Out*, pages 74–81, Barcelona, Spain. Association for Computational Linguistics.
- Shayne Longpre, Kartik Perisetla, Anthony Chen, Nikhil Ramesh, Chris DuBois, and Sameer Singh. 2021. [Entity-based knowledge conflicts in question answering](#). In *Proceedings of the 2021 Conference on Empirical Methods in Natural Language Processing*, pages 7052–7063, Online and Punta Cana, Dominican Republic. Association for Computational Linguistics.
- Junliang Luo, Tianyu Li, Di Wu, Michael Jenkin, Steve Liu, and Gregory Dudek. 2024. [Hallucination detection and hallucination mitigation: An investigation](#). *arXiv preprint arXiv:2401.08358*.
- Catherine Olsson, Nelson Elhage, Neel Nanda, Nicholas Joseph, Nova DasSarma, Tom Henighan, Ben Mann, Amanda Askell, Yuntao Bai, Anna Chen, et al. 2022. [In-context learning and induction heads](#). *arXiv preprint arXiv:2209.11895*.
- Pranav Rajpurkar, Jian Zhang, Konstantin Lopyrev, and Percy Liang. 2016. [SQuAD: 100,000+ questions for machine comprehension of text](#). In *Proceedings of the 2016 Conference on Empirical Methods in Natural Language Processing*, pages 2383–2392, Austin, Texas. Association for Computational Linguistics.
- Abigail See, Peter J. Liu, and Christopher D. Manning. 2017. [Get to the point: Summarization with pointer-generator networks](#). In *Proceedings of the 55th Annual Meeting of the Association for Computational Linguistics (Volume 1: Long Papers)*, pages 1073–1083, Vancouver, Canada. Association for Computational Linguistics.
- Dan Shi, Renren Jin, Tianhao Shen, Weilong Dong, Xinwei Wu, and Deyi Xiong. 2024a. [IRCAN: Mitigating knowledge conflicts in LLM generation via identifying and reweighting context-aware neurons](#). In *The Thirty-eighth Annual Conference on Neural Information Processing Systems*.
- WeiJia Shi, Xiaochuang Han, Mike Lewis, Yulia Tsvetkov, Luke Zettlemoyer, and Wen-tau Yih. 2024b. [Trusting your evidence: Hallucinate less with context-aware decoding](#). In *Proceedings of the 2024 Conference of the North American Chapter of the Association for Computational Linguistics: Human Language Technologies (Volume 2: Short Papers)*, pages 783–791, Mexico City, Mexico. Association for Computational Linguistics.
- Seungwoo Son, Wonpyo Park, Woohyun Han, Kyuyeon Kim, and Jaeho Lee. 2024. [Prefixing attention sinks can mitigate activation outliers for large language model quantization](#). *arXiv preprint arXiv:2406.12016*.
- Mingjie Sun, Xinlei Chen, J Zico Kolter, and Zhuang Liu. 2024. [Massive activations in large language models](#). *arXiv preprint arXiv:2402.17762*.
- Hugo Touvron, Louis Martin, Kevin Stone, Peter Albert, Amjad Almahairi, Yasmine Babaei, Nikolay Bashlykov, Soumya Batra, Prajjwal Bhargava, Shruti Bhosale, et al. 2023. [Llama 2: Open foundation and fine-tuned chat models](#). *ArXiv*, abs/2307.09288.
- Adam Trischler, Tong Wang, Xingdi Yuan, Justin Harris, Alessandro Sordani, Philip Bachman, and Kaheer Suleman. 2017. [NewsQA: A machine comprehension dataset](#). In *Proceedings of the 2nd Workshop on Representation Learning for NLP*, pages 191–200, Vancouver, Canada. Association for Computational Linguistics.
- Liam van der Poel, Ryan Cotterell, and Clara Meister. 2022. [Mutual information alleviates hallucinations in abstractive summarization](#). In *Proceedings of the 2022 Conference on Empirical Methods in Natural Language Processing*, pages 5956–5965, Abu Dhabi, United Arab Emirates. Association for Computational Linguistics.
- Shikhar Vashishth, Shyam Upadhyay, Gaurav Singh Tomar, and Manaal Faruqui. 2019. [Attention interpretability across nlp tasks](#). *arXiv preprint arXiv:1909.11218*.
- Jesse Vig and Yonatan Belinkov. 2019. [Analyzing the structure of attention in a transformer language model](#). In *Proceedings of the 2019 ACL Workshop BlackboxNLP: Analyzing and Interpreting Neural Networks for NLP*, pages 63–76, Florence, Italy. Association for Computational Linguistics.
- Tu Vu, Mohit Iyyer, Xuezhi Wang, Noah Constant, Jerry Wei, Jason Wei, Chris Tar, Yun-Hsuan Sung, Denny Zhou, Quoc Le, and Thang Luong. 2023. [Freshllms: Refreshing large language models with search engine augmentation](#). In *Annual Meeting of the Association for Computational Linguistics*.
- Han Wang, Archiki Prasad, Elias Stengel-Eskin, and Mohit Bansal. 2024. [Adacad: Adaptively decoding to balance conflicts between contextual and parametric knowledge](#). *arXiv preprint arXiv:2409.07394*.
- Wenhao Wu, Yizhong Wang, Guangxuan Xiao, Hao Peng, and Yao Fu. 2024. [Retrieval head mechanistically explains long-context factuality](#). *arXiv preprint arXiv:2404.15574*.
- Guangxuan Xiao, Yuandong Tian, Beidi Chen, Song Han, and Mike Lewis. 2024. [Efficient streaming language models with attention sinks](#). In *The Twelfth International Conference on Learning Representations*.

- Jiacheng Xu, Shrey Desai, and Greg Durrett. 2020a. [Understanding neural abstractive summarization models via uncertainty](#). In *Proceedings of the 2020 Conference on Empirical Methods in Natural Language Processing (EMNLP)*, pages 6275–6281, Online. Association for Computational Linguistics.
- Song Xu, Haoran Li, Peng Yuan, Youzheng Wu, Xiaodong He, and Bowen Zhou. 2020b. [Self-attention guided copy mechanism for abstractive summarization](#). In *Proceedings of the 58th Annual Meeting of the Association for Computational Linguistics*, pages 1355–1362, Online. Association for Computational Linguistics.
- Zhilin Yang, Peng Qi, Saizheng Zhang, Yoshua Bengio, William Cohen, Ruslan Salakhutdinov, and Christopher D. Manning. 2018. [HotpotQA: A dataset for diverse, explainable multi-hop question answering](#). In *Proceedings of the 2018 Conference on Empirical Methods in Natural Language Processing*, pages 2369–2380, Brussels, Belgium. Association for Computational Linguistics.
- Jia-Yu Yao, Kun-Peng Ning, Zhen-Hui Liu, Mu-Nan Ning, Yu-Yang Liu, and Li Yuan. 2023. Llm lies: Hallucinations are not bugs, but features as adversarial examples. *arXiv preprint arXiv:2310.01469*.
- Xiaowei Yuan, Zhao Yang, Yequan Wang, Shengping Liu, Jun Zhao, and Kang Liu. 2024. [Discerning and resolving knowledge conflicts through adaptive decoding with contextual information-entropy constraint](#). In *Findings of the Association for Computational Linguistics: ACL 2024*, pages 3903–3922, Bangkok, Thailand. Association for Computational Linguistics.
- Tianyi Zhang, Varsha Kishore, Felix Wu, Kilian Q. Weinberger, and Yoav Artzi. 2020. [Bertscore: Evaluating text generation with bert](#). In *International Conference on Learning Representations*.
- Haiyan Zhao, Hanjie Chen, Fan Yang, Ninghao Liu, Huiqi Deng, Hengyi Cai, Shuaiqiang Wang, Dawei Yin, and Mengnan Du. 2024. Explainability for large language models: A survey. *ACM Transactions on Intelligent Systems and Technology*, 15(2):1–38.
- Zifan Zheng, Yezhaohui Wang, Yuxin Huang, Shichao Song, Bo Tang, Feiyu Xiong, and Zhiyu Li. 2024. Attention heads of large language models: A survey. *arXiv preprint arXiv:2409.03752*.
- Wenxuan Zhou, Sheng Zhang, Hoifung Poon, and Muhao Chen. 2023. [Context-faithful prompting for large language models](#). In *Findings of the Association for Computational Linguistics: EMNLP 2023*, pages 14544–14556, Singapore. Association for Computational Linguistics.

A Prediction Uncertainty Analysis Details

A.1 Dataset and Sampling

We selected 6,000 samples from the MrQA training set (Fisch et al., 2019), distributed evenly across six sub-datasets. Each sub-dataset contained 500 correctly answered samples and 500 incorrectly answered samples, evaluated using the Exact Match (EM) metric.

A.2 Prompt and Decoding Settings

The Prompt 1 template (Yuan et al., 2024), as shown in Appendix G, was used for response generation. LLaMA2-7B (Touvron et al., 2023) served as the backbone model, with greedy decoding ensuring deterministic outputs.

A.3 Computation Process

For each sample, we calculated two metrics to quantify uncertainty. First, the **normalized entropy**, defined in Equation 1, measures the dispersion of probabilities across the vocabulary, providing an overall view of the model’s uncertainty. Second, the **top-1 token probability** represents the likelihood of the most probable token, offering a complementary perspective on the model’s prediction confidence. These metrics focus on the initial generated token to analyze how uncertainty affects response faithfulness.

A.4 Dataset and Sampling

We selected 6,000 samples from the training set (Fisch et al., 2019) for this analysis (The dataset consists of both the question and the context containing gold answer.). These samples were evenly distributed across six sub-datasets, with 1,000 samples drawn from each. For each sub-dataset, consisting of 500 correctly answered samples and 500 incorrectly answered samples (given context), the correctness of the responses is evaluated using the Exact Match (EM) metric.

A.5 Uncertainty Metrics Calculation Settings

We employed the Prompt 1 template (Yuan et al., 2024) (as shown in Appendix G) for generation with LLaMA2-7B (Touvron et al., 2023), using greedy decoding to ensure deterministic predictions. For each sample, we computed the normalized entropy of the distribution when the model generates the first answer token, while simultaneously recording the probability of the top-1 token in the distribution.

B Attention Signal Analysis Details

B.1 Dataset Construction

We constructed the dataset by selecting samples from the MrQA training set dataset (Fisch et al., 2019), focusing on cases where the model’s output changed from incorrect to correct after context concatenation. A total of 2,000 positive samples (utilized tokens) and 2,000 negative samples (non-utilized tokens) were selected. And each sample consists of a label (utilized or non-utilized token) and the corresponding attention ratio feature vector \mathbf{v}_j (under Prompt 1). The dataset was evenly split into training (50%) and testing (50%) sets.

B.2 Training and Evaluation

We trained a Logistic Regression (LR) classifier using 5-fold cross-validation. L2 regularization was applied to prevent overfitting. The classifier was evaluated across Transformer-based LLMs, including:

- LLaMA2: 7B, 13B, 7B-Chat, 13B-Chat
- Mistral: 7B, 7B-Instruct

C Details of LR Classifier Generalization and Feature Analysis

C.1 Cross-Prompt Test Results

To evaluate the robustness of the classifier under different prompts, we reconstructed the attention ratio feature vectors using Prompts 2, 3, and 4. These prompts differ in structure and phrasing but are consistent in task objectives. The classifier, trained using Prompt 1, was then tested on these alternative prompts.

The results, shown in Table 4, demonstrate that the classifier maintains an ACC exceeding 97% and AUC above 0.99 across all prompts. This indicates that the attention ratio signal is prompt-agnostic and generalizes well across different input structures.

| Prompt | LLaMA2-7B | | Mistral-7B | |
|---------|-----------|--------|------------|--------|
| | ACC | AUC | ACC | AUC |
| Prompt2 | 0.9797 | 0.9932 | 0.9762 | 0.9902 |
| Prompt3 | 0.9768 | 0.9926 | 0.9763 | 0.9889 |
| Prompt4 | 0.9794 | 0.9946 | 0.9771 | 0.9927 |

Table 4: Performance testing under different prompts. Training data: attention ratio feature vector under Prompt 1. Test data: attention ratio feature vector under Prompts 2, 3, and 4.

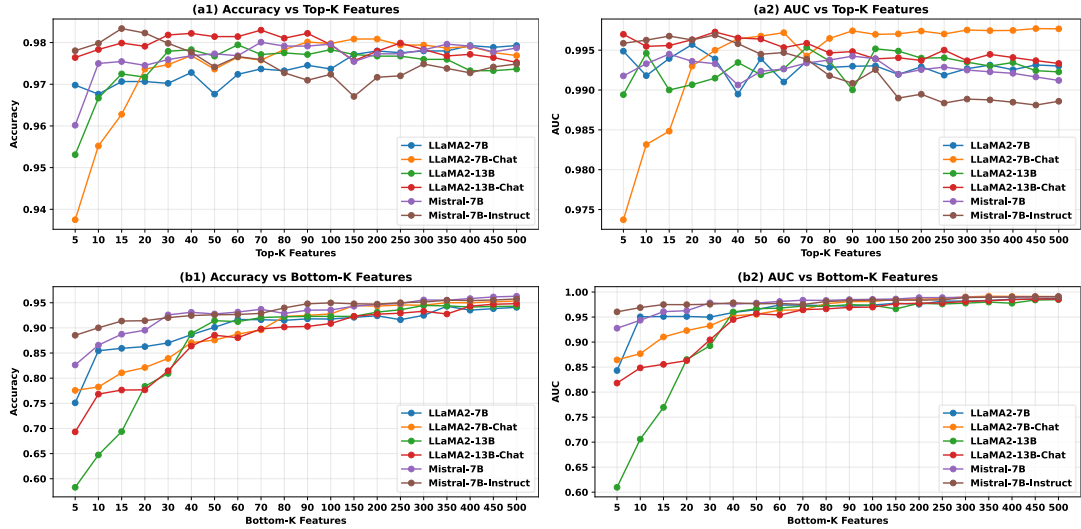


Figure 6: Performance of the LR classifier with Top- K and Bottom- K features. Based on the absolute values of feature coefficients, the Top- K and Bottom- K features were selected to train an LR classifier with sparse features. The figure shows the ACC and AUC performance of the classifier on the test set for different values of K .

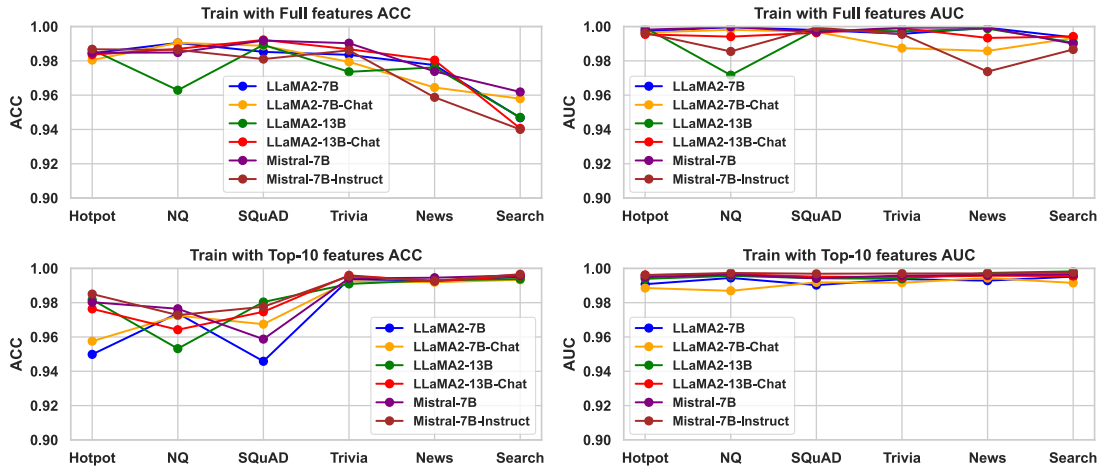


Figure 7: Out-of-domain performance of the LR classifier trained with full features and Top-10 features. Performance variations on out-of-domain data for LR classifiers trained using all features versus the top-10 features.

C.2 Analysis of the Importance of Different Features

In analyzing the LR classifier trained with attention values from all attention heads as features, we found that most feature coefficients had small absolute values. This indicates that only a few attention heads are crucial for utilization detection.

To explore their impact, we selected the top- K and bottom- K features based on the absolute values of their coefficients and trained LR models using these subsets. Figure 6: subplots (a1) and (a2) shows how classification accuracy (ACC) changes with K . Using top- K features, the model achieves over 0.95 accuracy for all LLMs with $K=10$, matching the performance of using all features. In contrast, models with bottom- K features

perform poorly, failing to reach 0.95 even with $K=100$. The AUC curves in Figure 6: subplots (b1) and (b2) for different K further confirm this. Models with top- K features maintain high accuracy and robustness, while those with bottom- K features show significantly worse performance. These results emphasize that a small number of key attention heads are enough for effective detection, while irrelevant features add little value and may introduce noise.

We also compared the performance of LR classifiers trained with all features versus only the top-10 features on out-of-domain data. As shown in Figure 7, the LR trained with only the top-10 features achieved better ACC and AUC on out-of-domain data.

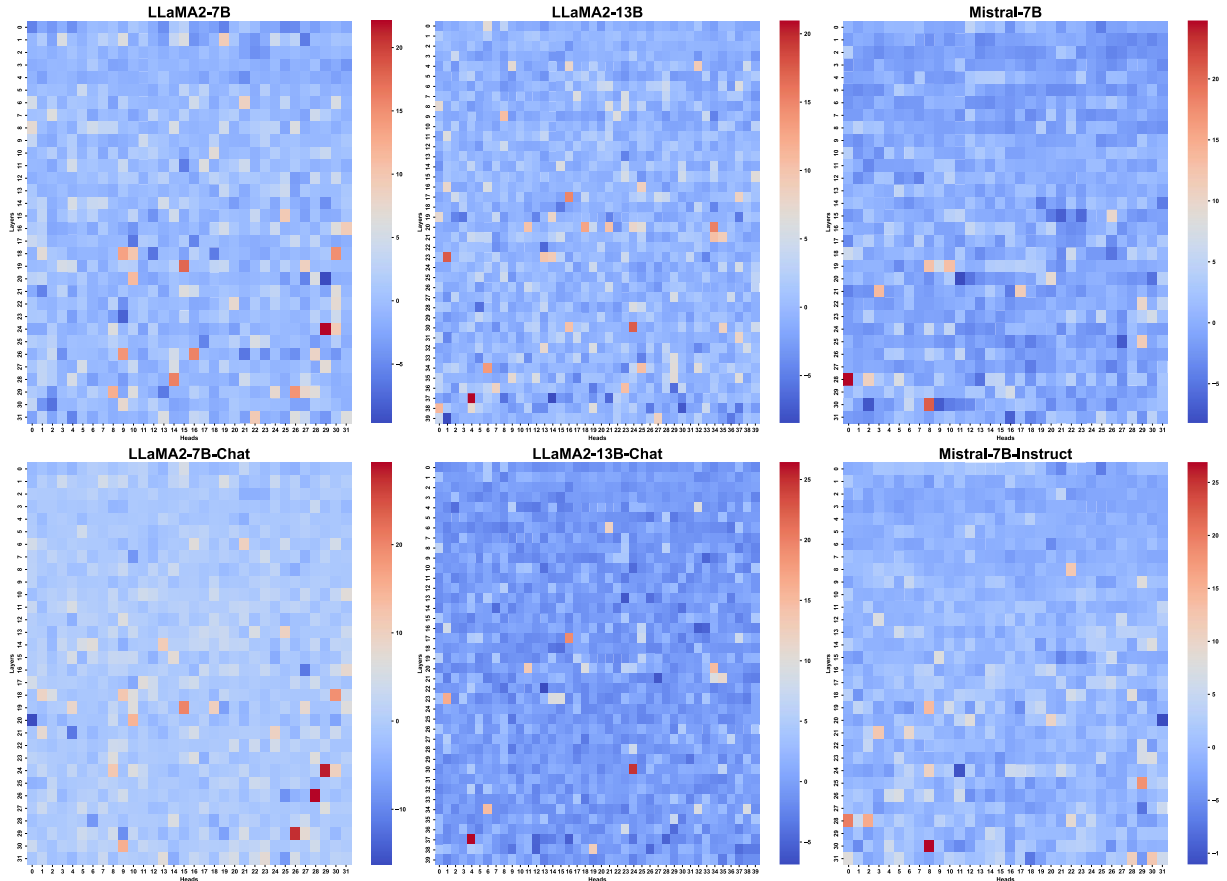


Figure 8: Heatmap of feature coefficients for LR. The heatmap of feature coefficients for LR classifiers trained using attention ratios from different LLMs as features.

Based on the ACC and AUC results, we find that **the LR classifier trained with the Top-10 features achieves good accuracy and robustness while using the minimum number of features.** Therefore, all subsequent inference employs LR classifiers trained with the Top-10 features.

D Analyzing Context Utilization Signal Contribution Across Heads

To further explore the role of attention heads in encoding contextual utilization signals, we conducted a detailed analysis to examine the strength and distribution of signals across heads. This section presents insights into the concentration of strong signals in certain heads, the independent utility of individual heads, and the complementarity of weaker heads.

D.1 Signal Strength and Concentration in Heads

To identify influential heads, we visualized the coefficients of the trained Logistic Regression (LR) classifier, which were derived from the attention

ratio features of all heads. Approximately 5% of the heads exhibited significantly high coefficients, suggesting that these heads dominate the classification task (Figure 8). Repeating this analysis across 100 random seeds revealed consistent selection of these top heads, indicating their robustness as key signal carriers.

To evaluate the standalone utility of these heads, we trained LR classifiers using the attention ratio from a single head as the feature. The results in Figure 9 show that About 5% to 10% of the heads achieved classification accuracies (ACC) above 0.8, highlighting their ability to independently encode contextual utilization signals. However, the majority of heads performed poorly in isolation, with ACCs below 0.8. This disparity emphasizes the varying degrees of utility across heads, with a small subset contributing disproportionately strong signals.

Additionally, we also observed that on the Mistral model, the vast majority of heads perform well when acting individually. This indicates **the presence of more high-performing heads in the Mis-**

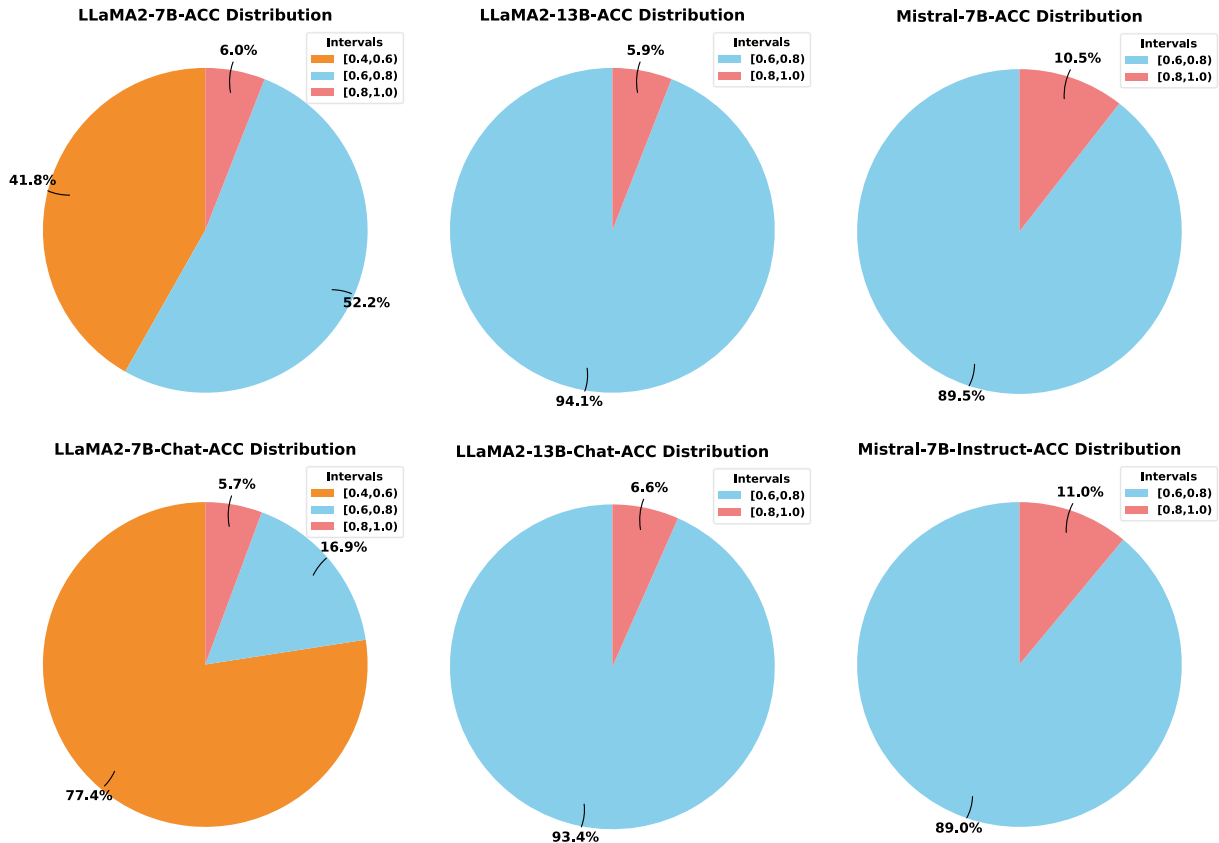


Figure 9: Performance distribution of LR with single features. An LR classifier is trained using the attention ratio from a single head as features. The figure shows the ACC distribution of LR classifiers trained with attention ratios from different heads on the test set.

tral model, which may explain why our method achieves greater improvements on Mistral compared to other models.

D.2 Complementary Contributions of Weaker Heads

Although most attention heads have limited standalone utility, we observe that combining weaker heads into subsets significantly improves classification performance. Figure 10 illustrates that we selected the bottom-K features, based on the classification accuracy of individual heads, to train the classifier and analyze the performance gain from combining weaker heads. The results show that when the number of bottom-K heads reaches 500, the classification accuracy stabilizes at approximately 90%. This finding highlights the complementarity of weaker heads, as their aggregated signals collectively achieve robust token classification.

D.3 Data-Dependent and Generalizable Heads

To investigate whether the influential heads identified in one dataset maintain their significance

across other datasets, we conducted cross-dataset experiments. For datasets A , B , and C , we analyzed the top 10 heads ranked by LR coefficients and observed significant differences in head rankings across datasets. However, when considering the intersection of the top 100 heads across all three datasets, we identified a subset of heads that consistently exhibited high importance.

Using this subset of generalizable heads, we re-trained the classifier on dataset A and tested it on datasets B and C . The model achieved high performance across all datasets, suggesting the presence of data-independent heads that encode universal contextual utilization signals. Conversely, dataset-specific top heads exhibited superior performance on their respective datasets, indicating a degree of data dependency in some heads' contributions.

Summary of Findings Our analysis reveals three key characteristics of attention heads in encoding contextual utilization signals:

1. **Concentration:** A small subset of heads consistently contributes strong independent signals, dominating the classification task.

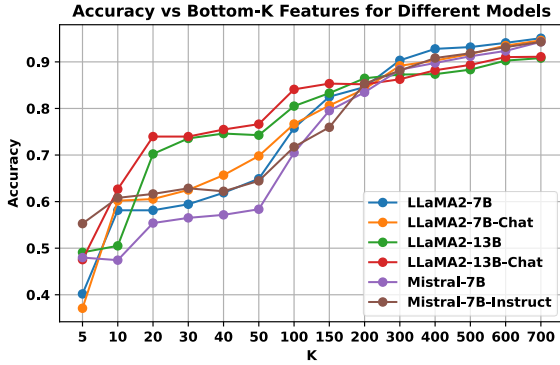


Figure 10: Performance of the LR classifier trained with Bottom- K features. Based on the ACC of LR classifiers trained using the attention ratio from a single head as features, the Bottom- K heads with the lowest ACC are selected. The LR classifier is then retrained using the attention ratios of these Bottom- K heads as features, and its performance on the test set is presented.

2. **Complementarity:** Weaker heads collectively provide complementary signals, enabling robust classification when aggregated.
3. **Data Dependency and Generalization:** Some heads exhibit data-specific importance, while others demonstrate generalizability across datasets, reflecting a balance between dataset-specific and universal contributions.

These findings highlight the nuanced roles of attention heads in contextual token utilization and provide a foundation for further exploration of their properties and applications.

E Models and Datasets

E.1 Model Details

The LLMs used in this work, along with its HuggingFace ID, is as follows:

- LLaMA2-7B: meta-llama/Llama-2-7b-hf
- LLaMA2-7B-Chat: meta-llama/Llama-2-7b-chat-hf
- LLaMA2-13B: meta-llama/Llama-2-13b-hf
- LLaMA2-13B-Chat: meta-llama/Llama-2-13b-chat-hf
- Mistral-7B: mistralai/Mistral-7B-v0.1
- Mistral-7B-Instruct: mistralai/Mistral-7B-Instruct-v0.1

F Experimental Details

The datasets used in this study include seven open-book question-answering (QA) datasets, grouped into three categories based on their QA task characteristics: multi-hop reasoning, long-form retrieval-based QA, and single-paragraph extraction tasks. Additionally, an adversarial dataset is included for evaluating the robustness of the proposed method. Detailed descriptions and dataset statistics are provided below.

F.1 Dataset Categories and Statistics

Multi-Hop Reasoning (HotpotQA). HotpotQA (Yang et al., 2018) is a benchmark dataset for multi-hop reasoning, requiring models to synthesize information across multiple paragraphs to generate an answer. This dataset emphasizes complex reasoning over distributed evidence, making it a critical benchmark for evaluating context utilization.

Long-Form Retrieval-Based QA (TriviaQA, SearchQA). TriviaQA (Joshi et al., 2017) and SearchQA (Dunn et al., 2017) require reasoning over longer contexts, with answers scattered across retrieved documents. These datasets test the model’s ability to focus on relevant content in lengthy contexts and generate precise answers.

Single-Paragraph Extraction (SQuAD). SQuAD (Rajpurkar et al., 2016), and NewsQA (Trischler et al., 2017) are standard extractive QA datasets where the answer is typically located within a single paragraph. These datasets are widely used for evaluating the span-extraction capabilities of QA systems.

Document-Level QA (NQ). NQ (Kwiatkowski et al., 2019) is a document-level open-domain question answering dataset driven by real user queries. It requires systems to extract long answers from entire Wikipedia documents and generate specific short answers, evaluating document-level information retrieval and natural language understanding capabilities.

Simulated Conflict Scenarios (NQ-Swap). NQ-Swap (Longpre et al., 2021) is an artificially constructed dataset that introduces adversarial entity swaps into NQ to create ambiguous or conflicting contexts. It evaluates the model’s ability to resolve conflicts and faithfully utilize context.

F.2 Dataset Sources and Formats

All datasets are standardized in the unified schema provided by the MrQA repository (Huggingface

ID: mrqa-workshop/mrqa), except for NQ-Swap, which is sourced from a separate repository (Huggingface ID: pminervini/NQ-Swap). The datasets used for training the logistic regression model (§ 2) and attention analysis (§ 3) are drawn from the training sets of the MrQA repository. Model performance evaluation is conducted using the validation sets from the same repository. All datasets have been preprocessed to ensure compatibility with our experimental framework.

F.3 Dataset Statistics

Table 5 presents the size of the datasets used in this study to evaluate model performance.

| Dataset | Number of Samples |
|--------------------------------|-------------------|
| HotpotQA (Multi-Hop) | 5904 |
| TriviaQA (Long-Form Retrieval) | 7785 |
| SearchQA (Long-Form Retrieval) | 16980 |
| SQuAD (Single-Paragraph) | 10507 |
| NewsQA (Single-Paragraph) | 4212 |
| NQ (Document-Level) | 12836 |
| NQ-Swap (Simulated Conflicts) | 4746 |

Table 5: Dataset statistics. A summary of the dataset sizes used for evaluation across different datasets.

F.4 Baseline Method Configurations

We implemented the baseline methods with their recommended hyperparameter settings for fair comparisons:

- **CAD** (Shi et al., 2024b): The contrastive adjustment factor α was set to 1.
- **COIECD** (Yuan et al., 2024): The entropy regularization parameter λ was set to 0.25, and the contrastive adjustment factor α was set to 1.

F.5 Implementation Details

All experiments utilized a unified prompt template (Prompt 1) to ensure consistency across methods. The prompt format is detailed in Appendix G. For decoding, greedy decoding was employed to produce deterministic outputs and facilitate direct comparisons across methods. All models run on NVIDIA A100 GPUs.

F.6 Results on Summarization Tasks

To validate the performance of our approach on long-form answer generation tasks, we conducted experimental evaluations on the CNN_DM (See et al., 2017) summarization dataset (we randomly

sampled 500 instances from the dataset for evaluation). Similar to prior work (Shi et al., 2024b), we adopted ROUGE-L (Lin, 2004), factKB (Feng et al., 2023), and BERTScore (Zhang et al., 2020) as comprehensive evaluation metrics to assess both the accuracy and factual consistency of the generated content. The experimental results, as shown in Table 6, demonstrate that our method achieves significant improvements on both the pretrained and chat versions of LLaMA2.

F.7 Additional Results of The Impact of Different α

We additionally evaluated the performance variations of our method on Mistral-7B and Mistral-7B-Instruct under different scaling factors α . Figure 11 illustrates the performance changes on the HotpotQA dataset. For Mistral-7B, the optimal performance is achieved at $\alpha = 5$. In contrast, for Mistral-7B-Instruct, the performance only stabilizes after $\alpha = 13$. This indicates that different models may require different optimal scaling factors for the best performance.

F.8 Impact of Different Prompts

To assess robustness to prompt variations, we tested multiple prompts from prior studies (Zhou et al., 2023; Yuan et al., 2024; Wang et al., 2024) (templates in Figure 13). Figure 12 illustrates the variations in F1 scores for LLaMA2-7B and Mistral-7B on the HotpotQA and NewsQA datasets under different prompt templates. The results show that DAGCD consistently outperforms baselines across all tested prompts, demonstrating its adaptability to diverse input formats and reliability across QA tasks.

G Prompt Templates

Figure 13 shows the prompt templates used in this paper.

H Symbol Explanation

The symbols and corresponding meanings defined in this paper, as shown in Table 7.

| Model | Decoding | ROUGE-L | factKB | BERT-P | BERT-R | BERT-F1 |
|----------------|-------------|---------------|---------------|---------------|---------------|---------------|
| LLaMA2-7B | Regular | 0.2081 | 0.9932 | 0.9000 | 0.7997 | 0.8465 |
| | CAD | 0.2361 | 0.9786 | 0.9054 | <u>0.8016</u> | <u>0.8514</u> |
| | COIECD | 0.2089 | 0.9845 | <u>0.9152</u> | 0.8014 | 0.8543 |
| | OURs | 0.2134 | <u>0.9856</u> | 0.9210 | 0.8026 | 0.8576 |
| LLaMA2-7B-Chat | Regular | 0.2368 | <u>0.9846</u> | <u>0.9056</u> | <u>0.8035</u> | <u>0.8515</u> |
| | CAD | 0.2082 | 0.9417 | 0.9001 | 0.7997 | 0.8466 |
| | COIECD | <u>0.2371</u> | 0.9807 | 0.9055 | 0.8034 | 0.8513 |
| | OURs | 0.2426 | 0.9866 | 0.9104 | 0.8036 | 0.8536 |

Table 6: Comparison of evaluation results on CNN/DailyMail. The table compares the evaluation results between greedy decoding and our proposed method on the CNN/DailyMail dataset. **Bold** denotes the best performance, while underlined indicates the second-best performance.

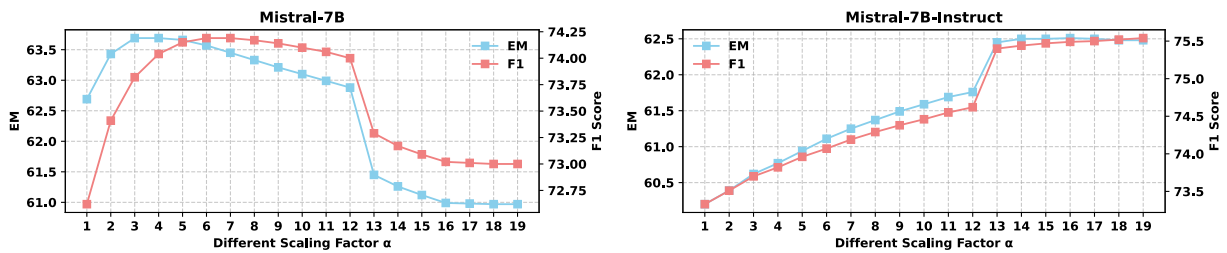


Figure 11: The performance on HotpotQA for DAGCD under different scaling factors.

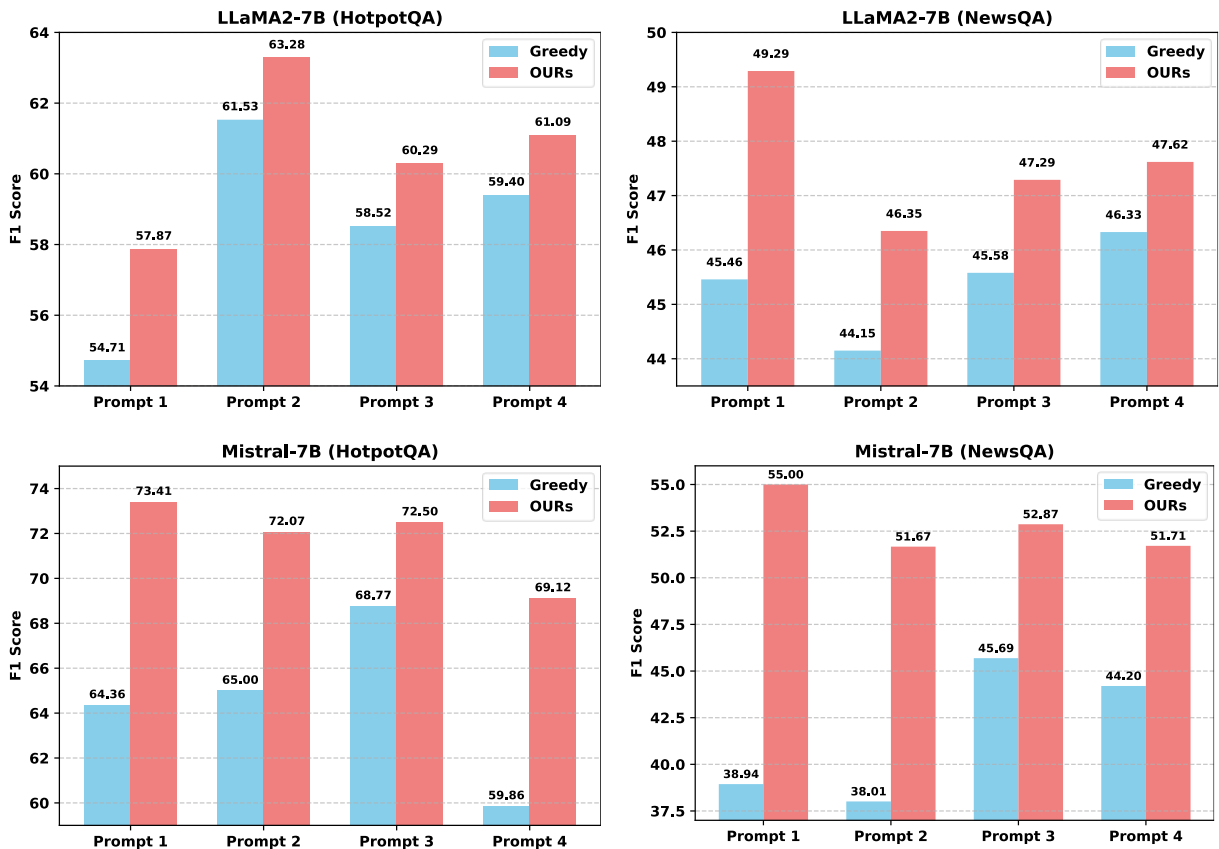


Figure 12: Performance variations across different prompt templates. The figure shows F1 score variations on the HotpotQA and NewsQA datasets for Greedy Decoding and OURs (DAGCD) under different prompt templates.

| | |
|--|--|
| <p>Prompt 1</p> <p>With Context: Given the following information: {context} Answer the following question based on the given information with one or few words: {question} Answer:</p> <p>Without Context: (for CAD and COIECD) Answer the following question based on your internal knowledge with one or few words: {question} Answer:</p> | <p>Prompt 2</p> <p>Given the following context, answer the question below: Context: {context} Question: {question} Answer:</p> <p>Prompt 3</p> <p>Read the given information and answer the corresponding question. {context} Question: {question} Answer:</p> <p>Prompt 4</p> <p>{context} Using only the references listed above, answer the following question: Question: {question} Answer:</p> |
|--|--|

Figure 13: Prompt templates used in this paper.

| Symbol | Meaning |
|----------------------|--|
| $H_{\text{norm}}(P)$ | Normalized entropy of distribution P |
| v_j | Attention ratio feature vector for token j |
| $v_j^{(K)}$ | Top-K attention ratio feature vector for token j |
| $a_{l,h}^j$ | The raw attention of the h -th head in the l -th layer for token j |
| $r_{l,h}^j$ | The attention ratio of the h -th head in the l -th layer for token j |
| s_j | The utilization score for token j |
| c_k | The coefficient of the k -th feature in the LR classifier |
| w_k | The normalized coefficient of the k -th feature in the LR classifier |
| U | The utilization distribution |
| u_i | The normalized utilization score for token j |
| U_{top} | The subset of U for tokens ranked in the top- R of the generation distribution |

Table 7: Annotation table.